1

Treatment of GM2 Gangliosidosis in Adult Sandhoff Mice using an Intravenous Self-Complementary Hexosaminidase Vector

Karlaina JL. Osmon¹, Patrick Thompson^{2,3}, Evan Woodley², Subha Karumuthil-Melethil⁴, Cliff Heindel⁴, John G. Keimel⁵, William F. Kaemmerer⁵, Steven J. Gray^{4,6,7} and Jagdeep S. Walia^{1,2,3,*}

¹Centre for Neuroscience Studies, Queen's University, Kingston, ON K7L 3N6, Canada; ²Department of Biomedical and Molecular Sciences, Queen's University, Kingston, ON K7L 3N6, Canada; ³Medical Genetics/Departments of Pediatrics, Queen's University, Kingston, ON K7L 2V7, Canada; ⁴Gene Therapy Center, University of North Carolina, Chapel Hill, NC, USA; ⁵New Hope Research Foundation, North Oaks, MN, USA; ⁶Department of Ophthalmology, University of North Carolina, Chapel Hill, NC, USA; ⁷Department of Pediatrics, University of Texas Southwestern Medical Center, Dallas, TX, USA

Abstract: *Background*: GM2 gangliosidosis is a neurodegenerative, lysosomal storage disease caused by the deficiency of β-hexosaminidase A enzyme (Hex A), an α/β -subunit heterodimer. A novel variant of the human hexosaminidase α -subunit, coded by *HEX M*, has previously been shown to form a stable homodimer, Hex M, that hydrolyzes GM2 gangliosides (GM2) *in vivo*.

Materials & Methods: The current study assessed the efficacy of intravenous (IV) delivery of a self-complementary adeno-associated virus serotype 9 (scAAV9) vector incorporating the *HEXM* transgene, scAAV9/*HEXM*, including the outcomes based on the dosages provided to the Sandhoff (SD) mice. Six-week-old SD mice were injected with either 2.5E+12 vector genomes (low dose, LD) or 1.0E+13 vg (high dose, HD). We hypothesized that when examining the dosage comparison for scAAV9/*HEXM* in adult SD mice, the HD group would have more beneficial outcomes than the LD cohort. Assessments included survival, behavioral outcomes, vector biodistribution, and enzyme activity within the central nervous system.

Results: Toxicity was observed in the HD cohort, with 8 of 14 mice dying within one month of the injection. As compared to untreated SD mice, which have typical survival of 16 weeks, the LD cohort and the remaining HD mice had a significant survival benefit with an average/median survival of 40.6/34.5 and 55.9/56.7 weeks, respectively. Significant behavioral, biochemical and molecular benefits were also observed. The second aim of the study was to investigate the effects of IV mannitol infusions on the biodistribution of the LD scAAV9/HEXM vector and the survival of the SD mice. Increases in both the biodistribution of the vector as well as the survival benefit (average/median of 41.6/49.3 weeks) were observed.

Conclusion: These results demonstrate the potential benefit and critical limitations of the treatment of GM2 gangliosidosis using IV delivered AAV vectors.

Keywords: Sandhoff, tay sachs, gene therapy, AAV, adeno-associated virus, hexosaminidase A, GM2 gangliosidosis, GM2 ganglioside.

ARTICLE HISTORY

Received: May 13, 2021 Revised: July 01, 2021 Accepted: July 16, 2021

DOI: 10.2174/1566523221666210916153051

1. INTRODUCTION

GM2 gangliosidosis is a group of neurodegenerative diseases characterized by the deficiency of β -hexosaminidase A enzyme (Hex A) to catabolize GM2 ganglioside (GM2), thereby causing GM2 accumulation within cellular lysosomes [1, 2]. In humans, Hex A is the sole enzyme capable

of catabolizing GM2 [2]. The lysosomal accumulation of GM2, which primarily occurs within neurons, leads to widespread neurodegeneration throughout the brain and spinal cord. Hex A is composed of two subunits, α and β , coded by the *HEXA* and *HEXB* genes, respectively [2]. Efficient hydrolysis of GM2 requires alignment of Hex A with a complex consisting of a GM2 Activator Protein (GM2AP) and GM2. Genetic mutations resulting in deficient activity of Hex A or GM2AP lead to the development of GM2 gangliosidosis diseases: Tay Sachs disease (TSD; α -subunit deficiency); Sandhoff disease (SD; β -subunit deficiency); or the AB-variant (GM2AP deficiency). The symptoms of the *infantile* TSD and SD include shakiness, rigidity, lethargy,

^{*} Address correspondence to this author at the Centre for Neuroscience Studies, Queen's University, Kingston, ON K7L 3N6, Canada; Department of Biomedical and Molecular Sciences, Queen's University, Kingston, ON K7L 3N6, Canada; Medical Genetics/Departments of Pediatrics, Queen's University, Kingston, ON K7L 3N6, Canada; E-mail: jagdeep.walia@kingstonhsc.ca

loss of motor control, seizures, and paralysis [2], and result in death by four years of age [3]. *Juvenile* and *Adult-onset* GM2 gangliosidosis have a delay in symptoms' onset due to low-level residual Hex A activity (~2-10% of normal activity) [4-6]. There are no curative treatments available for GM2 gangliosidosis.

In vivo gene transfer is a promising option for the treatment of neurological disorders caused by enzyme deficiencies [7-9]. Several studies have successfully utilized adeno-associated virus (AAV) vectors due to their ability to transduce neurons, demonstrated long-term expression within the Central Nervous System (CNS), low immunogenicity, and a small capsid size enabling better transport within the tissue. These studies have primarily investigated direct intraparenchymal vector administration [10-14] and have been shown to be effective in treating mouse models of GM2 gangliosidosis. While this method of delivery appears to distribute adequately across the small mouse brain, the distribution of the AAV vector in larger animals, even utilizing intraparenchymal convection-enhanced delivery, is primarily limited to the volume immediately surrounding the site of injection. This limited vector distribution could potentially impact the therapy effectiveness in larger animals and humans [15-18].

Previous preclinical gene therapy studies have had varying success in treating animal models of GM2 gangliosidosis [10-15, 19-31]. These previous studies used a variety of viral vectors, routes of administration, and treatment constructs, making a direct comparison to the current study using Hex M difficult. The transfer of the murine β-subunit transgene alone has been shown to be highly effective in rescuing mouse models of SD [19-21]. However, unlike humans, mice have an alternate biochemical pathway whereby a combination of sialidase and Hex B (the homodimer of the hexosaminidase β-subunit) catabolizes GM2 [32]. Because Hex B is unable to catabolize GM2 through this pathway in humans, the dose-response of gene transfer studies in mice that involve the expression of the murine hexosaminidase β -subunit could result in overly optimistic expectations for the translation for human clinical trials. Studies on mice involving gene transfer of both the murine α -subunit and the murine β -subunit are also subject to this uncertainty. It would be expected that in this case, the two expressed subunits would form the desired Hex A (heterodimer), but similar levels of Hex B might be formed due to the higher dimer stability of Hex B. Nevertheless, it may be noted that other studies delivered both hexosaminidase genes (α-subunit and β-subunit) in order to avoid depleting the supply of the endogenous complementary subunit [24]. The creation and use of the HEXM transgene have previously been reported by our team to circumvent this issue for murine studies [21, 22, 29], and allow for the packaging of a single self-complementary construct [21, 29]. The expressed μ-subunit homodimerizes to form the functional Hex M enzyme and would allow for the treatment of both TSD and SD in a single administration.

The efficiency of IV delivery of AAV vectors to the CNS has been reported to be significantly improved by the

use of self-complementary (sc) AAV genomes *versus* single-stranded (ss) [33] therefore, a self-complementary (sc) AAV vector is utilized in this study that expresses the previously described hexosaminidase μ -subunit, coded by *HEXM*, which is a synthesized variant of the human α -subunit [22]. This engineered variant of the human α -subunit incorporates enhanced dimer interface stability and a GM2AP binding site, which normally exists only on the hexosaminidase β -subunit. The μ -subunit homodimerizes to form a highly stable Hex M enzyme, previously shown to interact with the human GM2AP-GM2 complex and catabolize GM2 [22].

Achieving adequate biodistribution and cellular uptake is a major challenge for treating neurological diseases affecting broad regions of the CNS. Several AAV serotypes have been reported to cross the Blood-Brain Barrier (BBB), enabling transduction of CNS neurons and astrocytes [34-38]. The potential to obtain broad distribution throughout the CNS makes this minimally invasive intravenous (IV) route of delivery desirable. Recent studies have investigated IV delivered vector in SD mice but found long-term survival benefit only with neonatal injected mice in which the BBB has not yet fully formed [19-21]. The low permeability of the mature BBB limits the amount of vector from entering the CNS, and alternative viral vectors or methods of delivery appear to be needed to maximize the effectiveness of IV delivery.

In the current study, we investigated the efficacy of IV delivery of a scAAV9/HEXM vector to six-week-old adult Sandhoff mice. Mice were injected with one of two doses of the vector to investigate its potential benefit in terms of survival and behavioral outcomes. Survival and vector distribution were also investigated with the vector injection preceded by a fast IV injection of mannitol (3g/kg) intended to disrupt the BBB, temporarily increase its permeability, and enhance vector delivery to the CNS.

2. MATERIALS AND METHODS

2.1. Experimental Animals

The murine model of SD was obtained from Jackson Laboratory (stock number: 002914; B6;129S4-hexb^{ImTR/p}/J) and a colony for this study was maintained at Queen's University. Experimental mice were bred using female Hexb+/heterozygous and male Hexb-/- or female Hexb-/- heterozygous and male Hex-/- crosses. Genotype verification was performed through PCR amplification of deoxyribonucleic acid (DNA) extracted from ear punches [39-41]. All protocols were approved by the Queen's University Animal Care Committee.

2.2. rAAV Vector and Injections

The scAAV9/*HEXM* vector (Fig. 1) was produced at the vector core facility at the University of North Carolina as previously described [21, 29, 42]. The scAAV9/HEXM or scAAV9/*GFP* viruses were diluted to the correct volume in the vehicle (PBS with 350 mM total NaCl and 5% sorbitol)

as previously described [30]. Neonatal mice (postnatal day 0-1) received 50 μL with 2.5E+11 vg per mouse delivered through the temporal vein. Six-week-old mice received 100 μL of vector solution containing 1.0E+13 vector genomes (vg) per mouse (high dose, HD) or 2.5E+12 vg per mouse (low dose, LD) delivered *via* tail vein injections. Injections with either a LD or HD of scAAV9/*GFP* (Fig. 1) and PBS injections were also given as sham and untreated controls. A separate cohort of scAAV9/*HEXM* LD mice received a rapid injection of 25% mannitol at 3g/kg *via* the tail vein prior to the virus injection. Table 1 shows study design and cohort sizes.

2.3. Euthanizations and Tissue Processing

Mice were humanely euthanized either at 16-weeks of age or at their humane endpoint, defined by >15% weight loss and/or the loss of the righting reflex. All PBS and GFP cohorts were euthanized at 16 weeks to allow age-matched comparisons of hexosaminidase activity and GM2 ganglio-

side accumulation between treated groups and these controls. Visceral and nervous system organs were collected post-carbon dioxide asphyxiation, cardiac puncture, and perfusion using 10 mL of 1xPBS until clear. Visceral organs collected included the heart, lung, liver, kidney, spleen, gonad, and arm muscle. CNS tissue was grossly subdivided into 5 sections- rostral-, mid-, and caudal- section of the brain, and the cervical and lumbar spinal cord, as seen in Fig. (2) and as previously described [30]. Samples taken for histological purposes were deposited into 4% PFA for 24 hours, after which they were put into 70% ethanol until tissue embedding in paraffin. Samples taken for molecular and biochemical analysis were stored at -20°C for future processing. For further biochemical assessments, the MB samples were homogenized with 700 µL of PBS through three 10 second bursts of sonication. The samples were then spun down at 13000 RPM for 20 minutes at 4°C. 300 µL of the supernatant was separated for hexosaminidase activity assays, and the remainder of the supernatant and the precipitate was stored for future GM2 ganglioside storage analysis.

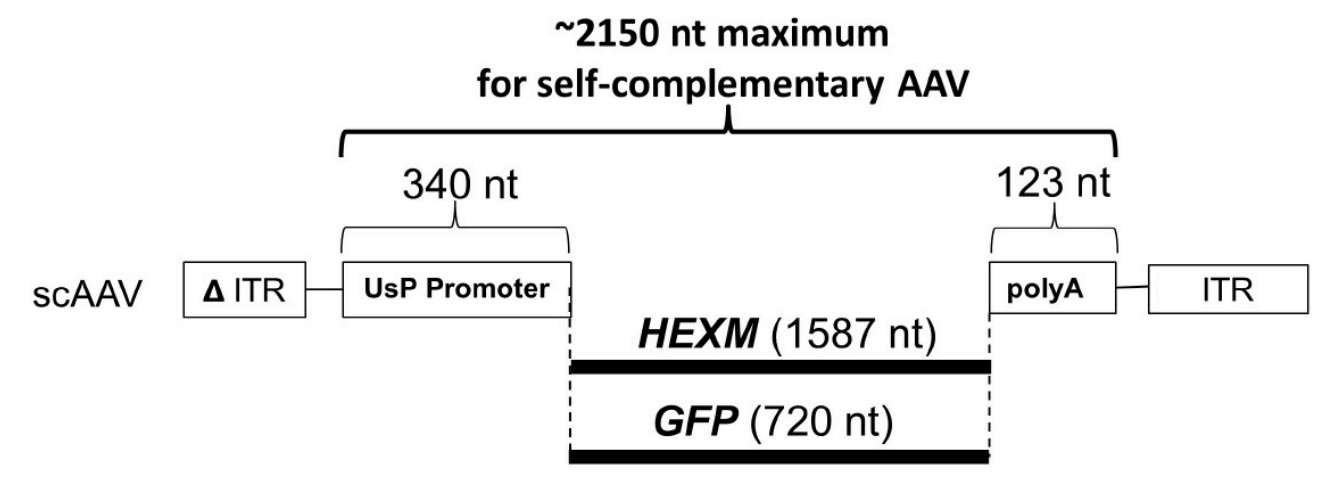


Fig. (1). AAV. HEXM vector design, with UsP promoter, as previously published [21].

Table 1. Study design.

Genotype	Treatment	Age of Administration	AAV Serotype	AAV Dose vg/Mouse	Number of Mice Terminated at 16- Weeks	Number of Mice Held to Long Term Humane Endpoint
Heterozygotes (+/-)	None	N/A	None	0	6	10
Sandhoff (-/-)	PBS	Adult	None	0	5	0
Sandhoff (-/-)	GFP	Adult	AAV9	1E13	4	0
Sandhoff (-/-)	GFP	Adult	AAV9	2.5E12	4	0
Sandhoff (-/-)	HEXM	Adult	AAV9	1E13	0	14
Sandhoff (-/-)	HEXM	Adult	AAV9	2.5E12	5	12
Sandhoff (-/-)	HEXM & Mannitol	Adult	AAV9	2.5E12	4	12
Sandhoff (-/-)	PBS	Neonatal	None	0	3	0
Sandhoff (-/-)	GFP	Neonatal	AAV9	2.5E11	4	0
Sandhoff (-/-)	HEXM	Neonatal	AAV9	2.5E11	6	8

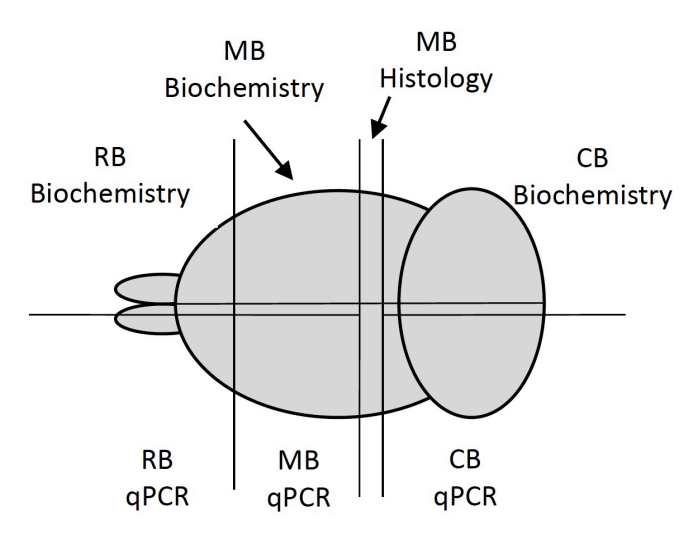


Fig. (2). Gross Sectioning of the Brain for Further Processing. Figure adapted from [30]. RB- Rostral section of the brain; MB- Midsection of the brain; CB- Caudal section of the brain. (*A higher resolution / colour version of this figure is available in the electronic copy of the article).*

2.4. Behavioral Testing

Behavioral assessments were performed weekly from 9 through 15 weeks of age, then monthly from 18 weeks until the humane endpoint of the animal. The Open Field Test (OFT) and Rotarod (RR) were conducted as previously described [21, 43]. Briefly, during the OFT, mice were monitored for general locomotion for 5 minutes with time moving being recorded by instrumentation (ActiMot; TSE Systems). In the RR, an accelerated protocol was used to assess coordination and strength in the mice over the course of a 5-minute trial, where the RPM at the time the mouse fell from the rod was recorded as "end RPM" (IITC Life Sciences, Series 8).

2.5. Hexosaminidase Activity Assay

Hexosaminidase activity assays were performed on MB samples utilizing the fluorogenic 4-methylumbelliferone (MU) substrates 4-methylumbelliferyl-2-acetamido-2-deoxy- β -D-glucopyranoside (MUG) and 4Methylumbelliferyl-7-6-sulfo-2-acetamido-2-deoxy-bD-glucopyranoside (MUGS) as previously described [21, 44, 45]. Samples of homogenized MB supernatant were diluted 1:50 μ l with PBS. The 4MU substrates were incubated with the diluted samples for 1 hour at 37°C, at which time the reaction was stopped using a 0.1M 2-amino-2-methyl-1-propanol (AMP) solution at a pH of 10.5. All hexosaminidase activity was normalized to galactosidase activity as measured by the 4-Methylumbelliferyl β -D-galactopyranoside (MUGal) substrate.

2.6. Vector Distribution Analysis

Vector biodistribution was determined through qPCR analysis as previously described [46]. Briefly, DNA extraction was performed on all organs collected. Isolated DNA

was then quantitatively analyzed using primers specific for the *GFP* and *HEXM* transgenes. Data are reported as the number of double-stranded target gene molecules per two double-stranded copies of murine *LaminB2*, approximating the amount of target gene per diploid cell. Primer sequences were as follows: *GFP* (forward: 5'-AGCAGCACGACTT CTTCAAGTCC-3'; reverse: 5'-TGTAGTTGTACTCCAGC TTGTGCC-3'); *HEXM* (forward: 5'-ACATCTACACCGCC-CAAGAC-3'; reverse: 5'-TTGACAGGGCCAAAAGTAC-C-3'); *LaminB2* (forward: 5'-GGACCCAAGGACTACCT-CAAGGG-3'; reverse: 5'-AGGGCACCTCCATCTCGGA AAC-3').

2.7. GM2 Assay

Extraction and separation of gangliosides from homogenized MB samples were performed as previously described [47-50]. Briefly, mixed gangliosides were extracted through a series of dilutions and evaporations under nitrogen in methanol and chloroform, then separated with a thin layer chromatography plate using a 50:45:10 chloroform: methanol:0.2% calcium chloride mobile phase. Visualization of the ganglioside bands was achieved by adding 0.4% orcinol solution in 25% sulfuric acid and baking the plate at 120°C for approximately 10 mins. Densitometry analysis of the bands was performed using Image J software. The intensity of the GD1A band served as an internal loading control for the intensity of the GM2 bands.

2.8. Histology

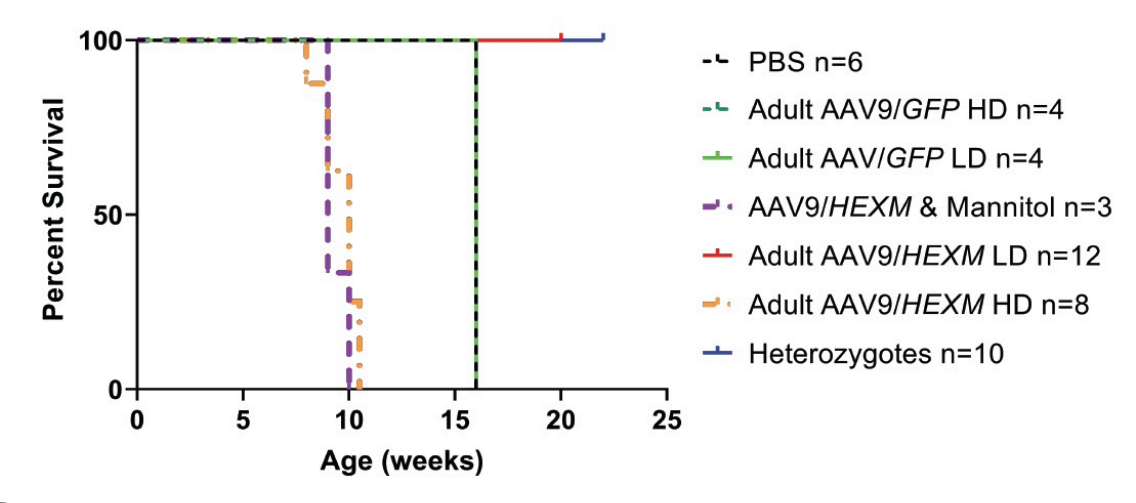
Histological analysis of the processed MBs was conducted as previously described [19, 21]. Briefly, the paraffinembedded samples were cut into 4-6µm sections and deparaffinized, then subjected to citrate buffer antigen retrieval. Slides were blocked for endogenous peroxidase activity and nonspecific binding, followed by incubations in primary and secondary antibodies. DAB stain was then applied prior to the dehydration and mounting of the slides. GM2 gangliosides were visualized through a 1:1000 dilution of the KM966 chimeric murine-human IgG1 anti-GM2 ganglioside antibody [51] (Kyowa Hakko Kirin Co. Ltd.), followed by incubation with a goat anti-human biotinylated secondary antibody.

2.9. Statistics

Statistical analyses were performed using GraphPad Prism and NCSS 12 statistical software. One-way ANOVAs using Tukey-Kramer post-hoc tests for multiple pairwise comparisons were performed on the MB hexosaminidase activity assays and Bonferroni post-hoc tests on the GM2 storage assays. Two-way repeated measure ANOVAs with Bonferroni post-hoc tests were used on behavioral measures. The behavioral analysis past 16 weeks was based only on the surviving mice. Kaplan–Meier curves were used to visualize improvement in the survival of the treated SD mice, with the significance of the observed improvements assessed by the Log-Rank (Mantel Cox) test. Mixed factors ANOVAs were performed to assess the biodistribution of the vectors

A

Premature Deaths within One Month Post-Injection



В

Long Term Survival of Intravenous Administration

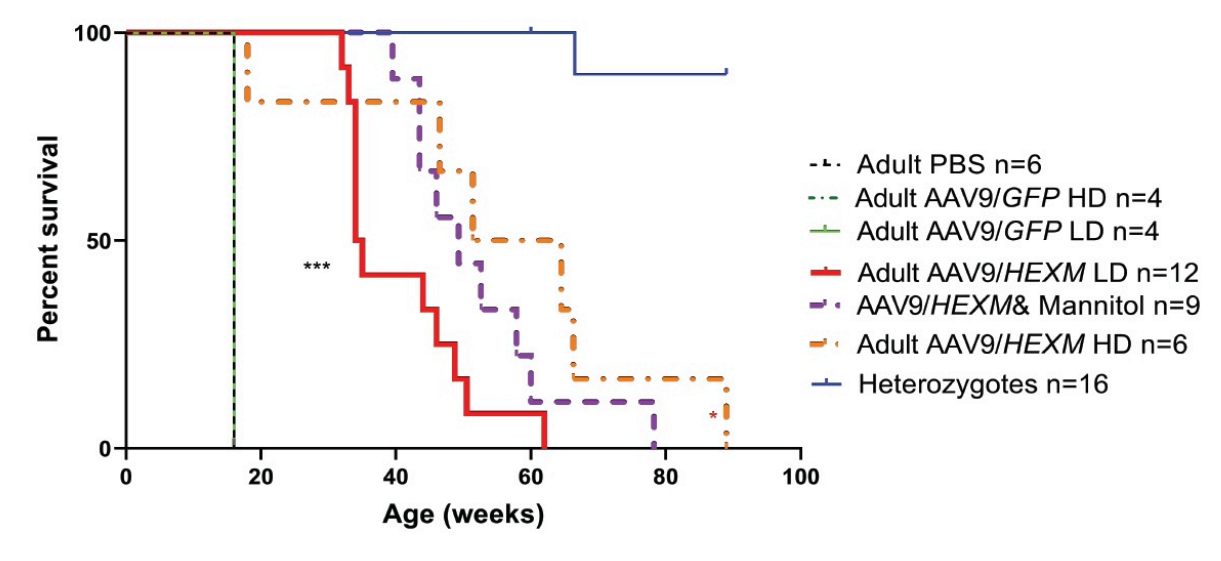


Fig. (3). Survival of the of the adult scAAV9/HEXM administrations. Some of the treatments displayed a bimodal survival curve, with either early death or prolonged survival. These have been separated into panels A and B. (A) Premature deaths within One Month Post-injection. The adult HD administration resulted in 57% lethality (8 of 14 mice) from acute toxicity in the month following the intravenous administration. In addition, 19% of the mice that received a co-injection of IV mannitol (3 of 16 mice) required euthanization within a month following injection. (B) Long term Survival. The average survival of the HD group (n=6, excluding the 8 that died acutely) was 56 weeks, a median of 56.7 weeks, with a range of 18 to 89 weeks. The average survival of the Adult LD (n=12) was 40.6 weeks, a median of 34.5 weeks, and a range of 32 to 62 weeks. The increase in survival of both the HD and LD adult cohorts was highly significant compared to the humane endpoint of the untreated mice (p<0.001), as per the Queen's University Animal Care Committee. The increase in survival of the HD group (excluding the acute toxicity) as compared to the LD administration was significant (p<0.05). The cohort of SD mice that received the co-infusion of the LD of scAAV9/HEXM and mannitol showed a significant increase in survival (mean of 41.6 weeks and range of 9.0 to 78.3 weeks) as compared to the natural survival of SD mice. However, this increase in survival was not significantly different from the cohort that received only the LD of the scAAV9/HEXM vector. (* = p<0.05, *** = p<0.001). (A higher resolution / colour version of this figure is available in the electronic copy of the article).

3. RESULTS

3.1. Survival

To verify vector transport across a more permeable, immature BBB, a cohort of neonatal mice were intravenously injected with scAAV9/HEXM via the temporal vein at a dose of 2.5E+11 vg per mouse. The average survival of this cohort (n=8) was 44.7 weeks, and their median survival was 46 weeks, with a range of 30-56 weeks of age (Supplementary Fig. **S1A**). The neonatal administration showed a highly significant survival benefit compared to the typical lifespan of approximately 16 weeks (R= 15-21 [40, 52, 53]; p<0.001).

In the HD injected adult mice (1.0E+13 vg/mouse), 8 of the 14 mice (~57% of the cohort) died shortly after the IV scAAV9/HEXM administration with their age at death ranging from 8 weeks to 10.5 weeks (Fig. 3A). The survival of the remainder of this cohort and mice in the other experimental cohorts is depicted in (Fig. 3B). The average survival of the Adult HD (n=6) and Adult LD (2.5E+12 vg/mouse, n=12) mice was 56.0 and 40.6 weeks of age, respectively. These Adult HD and LD groups had a median survival of 56.7 weeks and 34.5 weeks, and a range of 18-89 weeks and 32-62 weeks, respectively. Excluding the mice in the HD group that died shortly after vector administration, there was a highly significant increase in survival (p<0.001) of mice receiving either the HD or LD adult administrations as compared to the vehicle and GFP treated cohorts. In addition, there was a significant increase in the lifespan of the adult HD injected mice compared to the LD injected cohort (p<0.05).

Excluding the 3 mice that did not tolerate the mannitol co-injection (Fig. 3A), the survival of the LD & Mannitol co-hort (n=9) ranged from 39.5 to 78.3 weeks of age, with an average of 41.6 weeks and a median survival of 44.8 weeks (Fig. 3B). This was a significant increase in survival compared to untreated cohorts (p<0.01). However, co-administration of mannitol with the low dose of scAAV9/HEXM vector did not significantly increase the survival time of the mice compared to the mice receiving the low dose of scAAV9/HEXM alone (p = 0.0759).

3.2. Behavioral Outcomes

Behavioral locomotion and coordination were assessed in the adult scAAV9/HEXM SD cohorts through Open Field Test (OFT) and Rotarod (RR), respectively. From the age of 9 weeks through 15 weeks, there was a significant difference observed among treatment groups in the OFT time moving ($F_{6,35}$ =4.02, p<0.0001) (Fig. 4A). The adult HD group at 9 weeks spent less time moving compared to heterozygous controls (p<0.001). The adult HD group also spent less time

moving than the adult LD group at 9 weeks (p<0.05). Over the time-course from 18 to 30 weeks of age, there were no statistically significant differences between the locomotion of the remaining adult scAAV9/HEXM treatment groups (HD and LD) in the OFT.

The coordination of the scAAV9/HEXM treated cohorts was assayed through the accelerated protocol on the RR (F_5 , $_{33}$ =2.98, p=0.0250) (Fig. **4B**). From week 9 to week 22 of the behavioral testing time-course, the performance of the adult HD and LD cohorts approximated that of the heterozygote cohort. However, at the testing performed at the 26and 30-week timepoints, the adult LD cohort diverged from the heterozygote group, showing a significant decline in performance (p<0.01, p<0.05, respectively). The adult LD group also showed decreased coordination at 26 and 30 weeks compared to the adult HD cohort (p<0.001, p<0.001, respectively). The adult HD group outperformed the PBS cohort at 14 and 15 weeks (p<0.01, p<0.001, respectively). Likewise, the mice of the adult LD group were also more coordinated than the PBS group at 13, 14 and 15 weeks (p<0.05, p<0.01, p<0.001, respectively). The coordination of the heterozygote controls was significantly better than the untreated PBS cohort at 14 and 15 weeks (p<0.01, p<0.001, respectively).

The treated neonatal cohort also demonstrated increased general locomotion and coordination on the OFT and RR compared to the untreated cohorts (Supplementary Fig. S2).

3.3. Enzymatic Activity Assay

Hexosaminidase enzyme activity in the Midsection of the Brain (MB) homogenates was quantified using the synthetic fluorescent MUGS substrates relative to galactosidase activity measured with MUGal substrate. The analysis of variance of measures of hexosaminidase enzyme activity in MB tissue samples taken at termination showed a significant main effect of the group ($F_{6.18}$ =63.06, p<0.0001) (Fig. (5A); ratios were log-transformed for the statistical analyses to achieve homogeneity of variance among groups). At their long-term (humane) endpoint, the mice receiving scAAV9/HEXM at either the low dose or high dose had significantly greater hexosaminidase enzyme activity in their MB samples than control group mice receiving the scAAV/GFP (p < 0.001). There was also a dose effect, with the high dose group mice having significantly greater hexosaminidase enzyme activity in their MB samples than mice receiving the lower dose (p < 0.05). Hexosaminidase activity was also assessed in serum samples, where no increase in enzymatic activity was observed (data not shown).

Supplementary Fig. (S1B) provides the hexosaminidase activity analysis of the neonatal cohort.

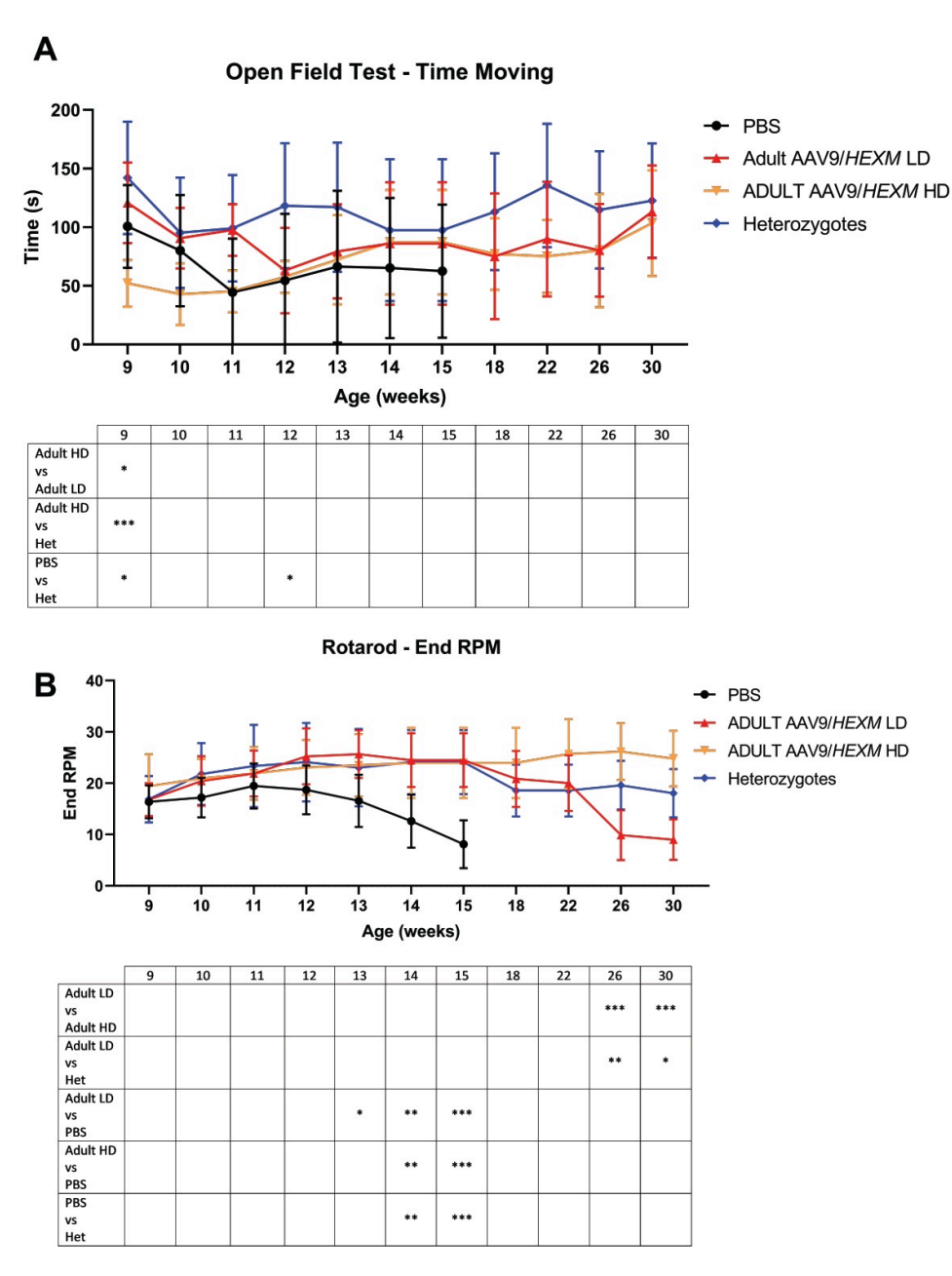


Fig. (4). Behavioral Analysis of the adult scAAV9/*HEXM* administrations. Statistics for PBS treated mice are not available beyond 15 weeks of age. Only comparisons with significance at any point during the time course of assessment are shown in the inlayed tables. (**A**) Open Field Test - Time Moving. From 9-15 weeks, there was a significant difference observed among treatment groups in the OFT ($F_{6,35}$ =4.02, p<0.0001). All scAAV9/*HEXM* treated animals did not have significant changes in their general locomotion compared to heterozygous controls (p>0.05), except for the Adult HD group at 9 weeks with a highly significant decrease in movement compared to Heterozygotes (p<0.001). Over the long-term time-course (18-30 weeks) there were no statistical differences between the locomotion of the treatment groups in the OFT. (**B**) Rotarod - End RPM. There was a significant effect of treatment observed ($F_{5,33}$ =2.98, p=0.0250). Over the time-course as measured in the RR, the coordination of all scAAV9/*HEXM* treatment groups approximated the activity of the heterozygous control mice until 26 and 30 weeks, where the Adult LD cohort diverged, showing a significant decline in performance as compared to heterozygous controls (p<0.01, p<0.05, respectively). The Adult LD group also showed decreased coordination at 26 and 30 weeks compared to the Adult HD cohort (p<0.001, p<0.001, respectively). In addition, the heterozygous controls performed significantly better than the untreated PBS cohort at 14 and 15 weeks (p<0.01, p<0.001, respectively), where the Adult LD group were also more coordinated than the PBS group at 13, 14 and 15 weeks (p<0.05, p<0.01, p<0.001, respectively). (* = p<0.05, ** = p<0.01, *** = p<0.001). (*A higher resolution / colour version of this figure is available in the electronic copy of the article*).

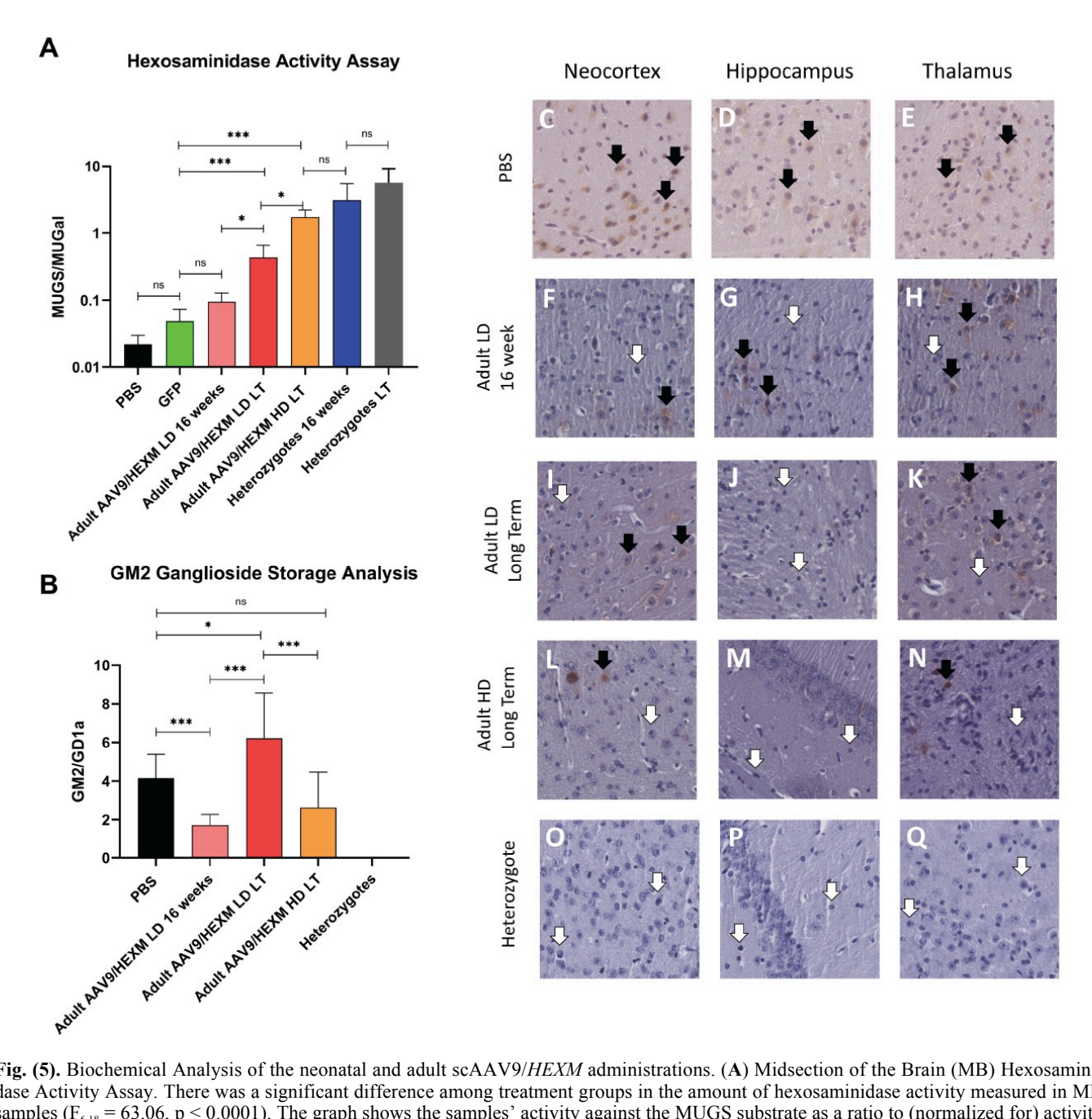


Fig. (5). Biochemical Analysis of the neonatal and adult scAAV9/HEXM administrations. (A) Midsection of the Brain (MB) Hexosaminidase Activity Assay. There was a significant difference among treatment groups in the amount of hexosaminidase activity measured in MB samples ($F_{6.18} = 63.06$, p < 0.0001). The graph shows the samples' activity against the MUGS substrate as a ratio to (normalized for) activity with the MUGal substrate. The differences between pairs of treatment groups shown in the graph and discussed in the text are based on the Tukey-Kramer method for multiple pairwise comparisons. (B) Ganglioside Storage Analysis. There was a significant effect of treatment group on the amount of GM2 ganglioside stored ($\bar{F}_{7,6}$ = 40.12, p<0.0001). The adult scAAV9/HEXM LD 16-week cohort showed a significant decrease in GM2 storage as compared to the PBS untreated group (p<0.001). A significant increase in the amount of GM2 stored was observed between the 16 week and LT timepoint for the adult scAAV9/HEXM LD cohort (p<0.001). As compared to the heterozygous controls, the PBS, GFP, adult scAAV9/HEXM LD LT, and the adult scAAV9/HEXM HD LT showed a highly significant increase in the amount of GM2 gangliosides stored (p<0.001), whereas the Adult scAAV9/HEXM LD 16 week group showed a significant increase (p<0.01). (C-Q) Histological Ganglioside Storage. Sections of the murine neocortex, hypothalamus, and thalamus from the PBS cohort (C-E), the AAV9/HEXM adult LD 16 week (F-H), and long term (I-K) cohorts, the AAV9/HEXM HD adult cohort (L-N), and the heterozygote controls (O-Q). Black arrows indicate GM2 ganglioside filled neurons, which were found predominantly throughout the PBS and adult longterm cohorts. The white arrows indicate similar neuron soma lacking the GM2 ganglioside accumulation. All images taken at 40x magnification. (* = p < 0.05, *** = p < 0.001, ns = not significant). (A higher resolution / colour version of this figure is available in the electronic copy of the article).

3.4. Ganglioside Storage Analysis

There was a significant effect of treatment on the amount of GM2 ganglioside stored ($F_{7.61}$ = 40.12, p<0.0001) (Fig. 5B). The Adult AAV9/HEXM LD 16-week cohort had significantly less GM2 storage compared to the PBS untreated group (p<0.001). The amount of GM2 gangliosides stored in the MB samples collected at the humane, longterm endpoint (LT timepoint) of the Adult scAAV9/HEXM LD cohort was significantly greater than that observed in the samples from the mice terminated at 16 weeks of age of this cohort (p<0.001). GM2 ganglioside storage in MB samples taken at the LT timepoint was significantly lower in the samples from the Adult HD group compared to the Adult LD cohort (p < 0.0001). Compared to the heterozygous controls, the PBS, Adult scAAV9/HEXM LD LT, and the Adult scAAV9/HEXM HD LT each showed a greater amount of GM2 gangliosides stored (p<0.001), as did the Adult scAAV9/HEXM LD group samples taken at 16 weeks (p<0.01). Supplementary Fig. (1C) shows the GM2 storage in the neonatal cohort.

Histological analysis showed noteworthy reductions of the GM2 ganglioside storage in the MBs of the adult LD and HD scAAV9/HEXM treatment groups (Fig. 5C-Q). Supplementary Fig. (3) depicts the histological analysis of the neonatal cohort.

3.5. Biodistribution Analysis of IV scAAV9/HEXM Treated Mice

The scAAV9/*HEXM* vector biodistribution for the adult intravenous administration cohorts was through qPCR analysis (Fig. 6A). Data are presented as the number of vector genomes per mouse genome. The biodistribution analysis of the 16-week and LT LD and HD scAAV9/*HEXM* administrations showed a similar distribution of the vector throughout the central nervous system. In addition, high copy numbers were seen in the heart and liver samples of all injected animals, similar to previous reports^{27,33}. Supplementary Fig. (S1D) shows the biodistribution analysis of the neonatal cohort

Compared to the LD cohort, the cohort that received a co-injection of mannitol with the vector showed a significant increase in the amount of vector uptake in all regions of the central nervous system (p<0.001) (Fig. **6B**). When assessing the biodistribution to peripheral organs, there was a significant interaction between the pattern of transgene detection across tissues depending upon the use of mannitol (p<0.05), with mannitol co-administration resulting in relatively greater *HEXM* DNA detected in the bicep and lung, and less in the heart and kidney, compared to the LD of vector alone.

4. DISCUSSION

This study demonstrated the efficacy of intravenous scAAV9/HEXM gene therapy in adult SD mice. Overall, the neonatal and adult LD and HD cohorts survived significantly longer than untreated controls, which correlated with the behavioral improvements. These improvements were also accompanied by significantly decreased GM2 storage and a significant increase in hexosaminidase activity in the MB tis-

sue samples. Additionally, the current study showed an increase in CNS vector genome distribution when the scAAV9/HEXM intravenous administration was paired with an intravenous mannitol injection, an agent that temporarily increases the passage of large molecules into the brain across the blood-brain barrier. This increase was not associated with longer survival of the mice, which may be due to the systemic nature of the disease in the SD mouse, whereby morbidity and mortality may be determined by a broader pathology than central nervous system effects alone.

HEXM gene transfer has been previously shown to effectively and significantly extend the lifespan and ameliorate phenotypic and biochemical measures in neonatal SD mice, and consequently, it has also been confirmed that this human Hex M enzyme effectively functions with the mouse GM2AP-GM2 complex to hydrolyze GM2 [21]. This neonatal treatment of SD mice with a therapeutic dose of 5E10vg/mouse of scAAV9.47/HEXM showed a 2.5 fold increase in survival of treated animals to a median of 40 weeks [21]. Unlike scAAV9, the scAAV9.47 used in the previous study was designed to de-targeted the liver [21, 54]. In comparison, the survival of the SD mice in the current study shows a median survival of 46 weeks in neonatal mice injected with 2.5E11vg/mouse of scAAV9/HEXM (using a 5-fold greater dose and an AAV9 serotype which is different than the AAV9.47 serotype previously used). Adult stage injections of scAAV9/HEXM had not been studied previously. In this study, the increase in survival of the treated adult SD mice demonstrates the effectiveness of the scAAV9/HEXM vector to be distributed within the CNS. Excluding the deaths that occurred within one month following the vector injection, the adult HD cohort had a 3.5-fold increase in survival benefit, while the adult LD cohort showed a 2.5-fold increase in survival, as compared to the natural SD mouse survival. However, this increase in survival came at the cost of acute toxicity in the month following administration of the HD of the vector. The percentage of animals succumbing to acute toxicity implies that the 1E13 vg/mouse dose is approximately the lethal dose (LD50) for this vector. Although it was investigated, the cause of death of these mice was not conclusively determined. The timing of the acute toxicity coincides with the timing of maximal gene expression, potentially implicating the HexM protein itself. Alternatively, the timing is consistent with the cause being an immune response to either the AAV9 capsid protein or overproduced HexM protein, or both. There was an increase in liver enzyme levels in samples from animals, but the histopathological analysis did not identify liver damage. Analysis of serum samples for liver enzyme levels was not possible in all animals because some were found to have died overnight, preventing the collection of useful samples. There were no early deaths or observed clinical toxicity in the four mice injected with the HD of the scAAV9/GFP vector or in the 17 mice injected with the LD of the scAAV9/HEXM vector. Other studies have reported severe immune responses to high doses of AAV administered by intravenous infusions [55] or by direct brain intraparenchymal injections [56]. The lack of increased hexosaminidase levels in the blood (while tissue levels are increased) may be suggestive of an antibody response against Hex M (data not shown). Hex M is a variant of the human Hex A protein and is secreted from transduced cells, which may make it more immunogenic than GFP. A study investigating the possibility of an anti-Hex M immune response, and whether a prophylactic immune suppression regimen may ameliorate such acute toxicity, is underway in our lab.

GM2 ganglioside accumulation begins weeks or months before the primary symptoms of SD become apparent [14, 57]. Administration of the AAV9/HEXM vector at a later age still conveys significant benefit, *i.e.*, Neonatal vs Adult.

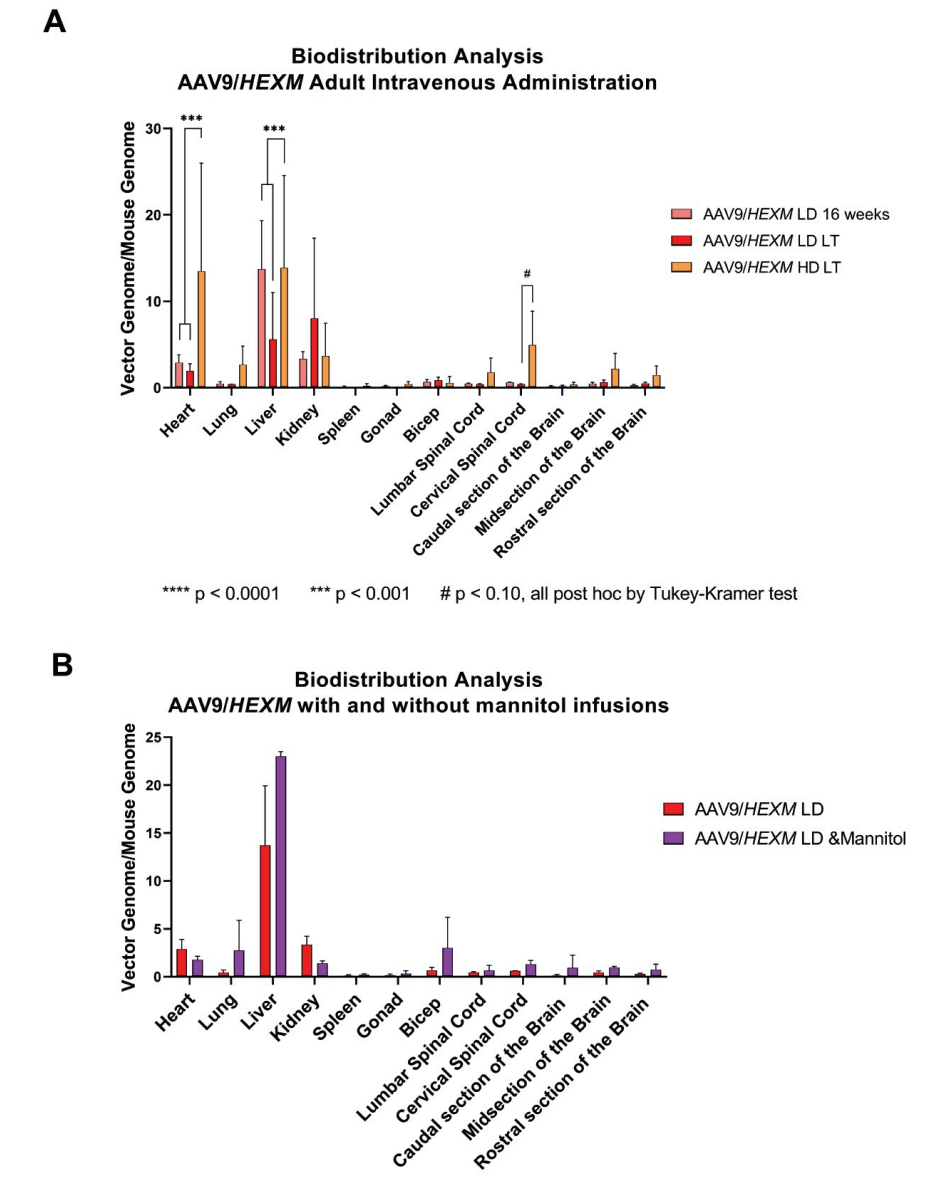


Fig. (6). Copy Number Analysis for Biodistribution of the scAAV9/*HEXM* Vector. Presented as the number of vector genomes per diploid mouse genome. (**A**) The biodistribution for the LD cohort at 16 weeks and long term, as well as the HD long term cohort. There was a significant effect of scAAV9-HexM dose on the copy numbers of HexM DNA found in the heart (p < 0.001) and liver (p < 0.01) of mice at their humane endpoint, with greater copy numbers found in the higher dose group. A repeated measures ANOVA showed a significantly higher number of copies in the CNS of mice receiving the higher dose *versus* those receiving the lower dose (p < 0.05) when considering the CNS regions collectively. Post hoc tests on a region-by-region basis were not significant; however, the data suggest that the dose effect was likely greatest in the region of the cervical spinal cord (p < 0.10). (**B**) The inclusion of the mannitol infusion with the LD scAAV9/*HEXM* significantly increased the vector biodistribution across the central nervous system compared to the LD virus alone (ANOVA with one between animal factor [mannitol or not] and one within animal factor [region of CNS], mannitol main effect: p < 0.001). However, no *post hoc* test for mannitol effect at individual CNS regions achieved significance). When assessing the non-central nervous system organs, there was a significant interaction between the pattern of transgene detection across tissues depending upon the use of mannitol (p < 0.05), with mannitol co-administration resulting in relatively greater *HEXM* DNA detected in the bicep and lung, and less in the heart and kidney, compared to the LD alone. (*A higher resolution / colour version of this figure is available in the electronic copy of the article*).

Previous behavioral studies have demonstrated that SD mice exhibit a decrease in measures of strength, coordination and general locomotion [21, 39, 40, 53]. The current study also found a decline over time in phenotypic performance consistent with previous findings for the untreated SD mice [19, 23, 40]. In contrast, the adult LD and HD scAAV9/HEXM treated mice exhibited a long-lasting improvement in performance on the Rotarod as compared to untreated controls. The HD scAAV9/HEXM cohort exhibited significantly better performance than untreated SD mice, and sustained this level of performance throughout the entire 30-week testing period, whereas the LD group performed better than untreated SD mice and did not begin exhibiting a decline in coordination and strength as measured on the rotarod until 26-week testing (Fig. 4B). Then, the decline in the performance of the LD group approximated the drop-off in performance seen earlier in the untreated SD mice.

The GM2 ganglioside storage analysis conducted in the current study is consistent with that of previously reported levels [19, 21]. The adult LD groups showed decreased GM2 ganglioside storage compared to both age-matched untreated groups (GFP/PBS) and their LD counterparts assessed at the long-term timepoint (humane endpoint). This demonstrates that the increase in enzyme activity in adulthood was able to degrade GM2 and reduce GM2 accumulation, and therefore affect the course of the disease.

It has been theorized that raising the cellular enzyme activity levels in lysosomal storage disease above a 'critical enzyme threshold', roughly above 10-15% of the normal enzyme activity level, will be sufficient to cure the disease due to the phenomenon of metabolic cooperation or cross-correction [4, 6]. Metabolic cooperation occurs when the therapeutic enzymatic product is secreted by successfully transduced cells and can then be taken up by surrounding non-transduced cells [4, 6]. In this study, mice receiving the low dose of scAAV9/HEXM had a level of hexosaminidase enzyme activity in their MBs, averaging 13.9% of the level found in the MBs of heterozygous mice at 16 weeks of age. Mice receiving the high dose (and surviving the acute toxicity period) had a level of hexosaminidase enzyme activity in their MBs, averaging 55.9% of the level of 16-week-old heterozygotes. The increase in these average levels of Hex activity was sufficient to provide a survival benefit, but it was not sufficient to enable the mice to live to a normal lifespan (Fig. 3), (Supplementary Fig. S1A). However, it should be noted that these are the average activity levels across a varied population of cells from the MB samples and may not be indicative of the enzyme activity within individual cells or more discrete CNS regions.

It was noted that there was higher hexosaminidase activity in the long-term LD cohort than in the 16-week cohort, but there was also more GM2 accumulation in the 16-week cohort than the LT cohort. The approach to the critical enzyme threshold could explain this discrepancy. Below 10-15% of normal hexosaminidase activity, there is still catabolism of the GM2 substrate; however, the GM2 substrate is still accumulating too quickly for the 10-15% en-

zyme activity to handle. From the time the mice were administered the treatment, Hex M was working to decrease the rate at which the GM2 ganglioside was accumulating. At the 16 week endpoint, unlike their untreated control counterparts, the mice comprising the LD cohort were asymptomatic due to the increase in enzyme activity provided by the scAAV9/HEXM treatment, which in turn worked at decreasing the rate of GM2 accumulation (Fig. (5B), PBS in black vs LD 16 week in pink). The long term LD cohort showed relatively high levels of GM2 accumulation compared to the 16 week LD and PBS cohorts (Fig. (5B), LD LT in red compared to the PBS in black and LD 16 week in pink), likely because the rate at which the Hex M activity was able to catabolize GM2 in the LD LT mice was sufficient to significantly extend the life of the animals, but still showed a very slow disease progression towards symptomatic SD, where the accumulation of GM2 in these mice significantly exceeded the load of that found within the PBS controls. As for the difference between the hexosaminidase activity between the 16-week and long-term timepoints, as the enzyme activity is normalized to an endogenous control, assuming that at 16 weeks, asymptomatic treated animals have very little neurodegeneration, there is a dilution of the amount of Hex M across all brain cells, whereas the symptomatic long-term mice have undergone severe neurodegeneration and it is likely that only those cells and their immediate neighbors producing the Hex M would remain, increasing the signal to the endogenous background measured in this group.

The biodistribution of the scAAV9/HEXM treatment in the adult mice was noted to be similar between animals terminated at 16 weeks and those terminated at long-term (humane endpoint) timepoints. This suggests there was little to no elimination of vector genomes from animals from the 16week timepoint onwards. In addition, a similar presence of the vector genome throughout the brain and spinal cord tissues of all adult and neonatal treated mice was observed, indicating that the scAAV9/HEXM vector crossed both the mature (in 6-week-old mice, (Fig. 6A)) and immature blood--brain barrier (in neonates, Supplementary Fig. S1D). There was a significant effect of scAAV9/HEXM dose on the copy numbers of *HEXM* DNA found in the heart (p < 0.001) and liver (p < 0.01) of mice at their humane endpoint, with greater copy numbers found in the higher dose group. Among mice that received the lower dose of scAAV9-HEXM, there were significantly fewer copies of HEXM DNA found in the livers of mice at their humane endpoint, compared to the copies in the livers of the mice that were terminated at 16 weeks of age. A repeated-measures ANOVA showed a significantly higher number of copies in the CNS of mice receiving the higher dose *versus* those receiving the lower dose (p < 0.05) when considering the CNS regions collectively. Post hoc tests on a region-by-region basis were not significant; however, the data suggest that the dose effect was likely greatest in the region of the cervical spinal cord (p < 0.10). A significant increase in uptake and persistence of the scAAV9/HEXM vector by a factor of 2.34-fold throughout the central nervous system was seen when the IV LD administration was paired with mannitol (Fig. 6B). This

is consistent with the expected effect of mannitol on the blood-brain barrier [15-18].

Intracarotid delivery of a high dose of a hyperosmotic agent has been shown to disrupt the ipsilateral BBB and enable the transport of therapeutic agents into the CNS from the bloodstream [15-18]. Both mannitol and arabinose are commonly used as hyperosmotic agents in animal studies. Intravenous mannitol is currently approved for human use by the US Food and Drug Administration (FDA) and is labeled for the reduction of intracranial pressure and brain mass.

The use of mannitol to reduce intracranial pressure has been performed in clinical and pre-clinical settings [16, 17, 58-62]. The administration of intra-arterial injection of 25% wt/vol of mannitol followed by the gene therapy treatment 2 minutes later [62] showed that the optimal time in which to deliver a therapeutic after the mannitol has been delivered to disrupt the BBB is 0-5 minutes, where a minimum period of hyperosmolarity is required for sufficient BBB disruption.

While the current study showed an increase in CNS vector uptake when preceded by a mannitol injection (rapid IV, total fluid volume of 25% mannitol) plus the hyperosmolarity of the vector vehicle may have been excessive for the three mice that required humane euthanizations within a month following vector injection. A similar study used 25% mannitol at a dose of 1-2 mg/g of the mouse to facilitate the movement of a gene therapy treatment across the BBB [61], which is lower than the dose used in the current study (3 g/kg = 3 mg/g mouse). Further investigation of the dose and route of mannitol delivery (e.g., intracarotid) is required to identify a safe and effective means of enhancing AAV vector transport across the BBB.

Previous studies utilizing AAV gene therapy have reported high incidences of hepatic or lung tumors [19, 63-65]. Throughout the course of this study, we did not encounter any tumors. This may be due to the synthetic promoter used in the scAAV9/HEXM treatment that confers moderate levels of expression since it has been shown that tumorigenicity can be promoter dependent correlating with stronger expression [66]. The immunological and toxicological effects of the vectors require further assessment.

CONCLUSION

In the current study, we investigated the efficacy of 2 different doses on the adult administration of AAV9/HEXM in the SD mice. The data obtained support our hypothesis of a dose-response to scAAV9/HEXM; namely, that a higher dose can confer a greater benefit than a lower dose. However, this support was limited to mice that did not have a toxic acute reaction to the higher dose. With a dose of 1E13 vg/mouse (HD), there was an approximate 57% lethality, as shown in Fig. (3A). Excluding the mice lost to acute toxicity from the adult HD cohort, there was an increase in survival, behavior, biochemical and molecular outcomes when comparing HD and LD adult injected groups. Excluding the acute toxicity, we noted that in these adult mice, with a 4x dosage increase, there was a 1.44x increase in survival bene-

fit and an increase in brain hexosaminidase activity. The adult LD and HD cohorts showed 2.5-fold and 3.7-fold increases in survival over the natural lifespan of SD mice (Fig. **3B**). The adult HD group outperformed the adult LD cohort throughout the behavioral testing, including the 26- and 30-week testing timepoints, when the LD cohort began declining in its coordination measures on the RR (Fig. **4B**). There was substantially less GM2 ganglioside in both the neonatal and adult scAAV9/HEXM recipients, as compared to the accumulation seen in the PBS treated group (Supplementary Fig. **S1C** and Fig. **5B**). Molecular analyses demonstrated the vector's ability to cross the blood-brain barrier and distribute it across the brain and spinal cord (Fig. **6**).

While the current study clearly shows that the scAAV9/HEXM vector can be effective in treating SD mice, further investigations are warranted into the toxicology of the treatment as well as optimizing a method of delivering gene vectors to the CNS to safely maximize treatment efficacy with minimal side effects. Future studies may also investigate the use of non-viral gene replacement methods [67]. Nevertheless, this study provides a solid step towards the translation and justification of a future clinical trial of scAAV9/HEXM gene therapy for TSD and SD.

ETHICS APPROVAL AND CONSENT TO PARTICIPATE

All protocols were approved by the Queen's University Animal Care Committee (Walia-2013-016), Canada.

HUMAN AND ANIMAL RIGHTS

No humans were used in this study. All experiments on animals were conducted in accordance with the Queen's University Animal Care and the Canadian Council on Animal Care guidelines and can be found athttps://www.queensu.ca/animals-in-science/.

CONSENT FOR PUBLICATION

Not applicable.

AVAILABILITY OF DATA AND MATERIALS

Not applicable.

FUNDING

This study was funded by the New Hope Research Foundation (to J.W., and S.G.).

CONFLICT OF INTEREST

S. Gray has received patent royalties from Asklepios Biopharma for technologies not directly linked to this study. The UsP promoter intron is patented by inventor J. Keimel. The rest of the authors have no competing financial interests.

ACKNOWLEDGEMENTS

We thank Kyowa Hakko Kirin Co. for graciously providing the KM966 antibody.

SUPPLEMENTARY MATERIAL

Supplementary material is available on the publisher's website along with the published article.

REFERENCES

- [1] Sandhoff K. My journey into the world of sphingolipids and sphingolipidoses. Proc Jpn Acad, Ser B, Phys Biol Sci 2012; 88(10): 554-82. http://dx.doi.org/10.2183/pjab.88.554 PMID: 23229750
- [2] Sandhoff K, Harzer K. Gangliosides and gangliosidoses: principles of molecular and metabolic pathogenesis. J Neurosci 2013; 33(25): 10195-208. http://dx.doi.org/10.1523/JNEUROSCI.0822-13.2013 PMID: 23785136
- [3] Mahuran DJ. Biochemical consequences of mutations causing the GM2 gangliosidoses. Biochim Biophys Acta BBA - Mol Basis Dis 1999; 1455(2): 105-38. http://dx.doi.org/10.1016/S0925-4439(99)00074-5
- [4] Conzelmann E, Sandhoff K. Biochemical basis of late-onset neurolipidoses. Dev Neurosci 1991; 13(4-5): 197-204. http://dx.doi.org/10.1159/000112160 PMID: 1817024
- [5] Conzelmann E, Sandhoff K. Partial enzyme deficiencies: residual activities and the development of neurological disorders. Dev Neurosci 1984; 6(1): 58-71.
- [6] Leinekugel P, Michel S, Conzelmann E, Sandhoff K. Quantitative correlation between the residual activity of β-hexosaminidase A and arylsulfatase A and the severity of the resulting lysosomal storage disease. Hum Genet 1992; 88(5): 513-23. http://dx.doi.org/10.1007/BF00219337 PMID: 1348043
- [7] Weinberg MS, Samulski RJ, McCown TJ. Adeno-associated virus (AAV) gene therapy for neurological disease. Neuropharmacology 2013; 69: 82-8. http://dx.doi.org/10.1016/j.neuropharm.2012.03.004 PMID: 22465202
- [8] Hocquemiller M, Giersch L, Audrain M, Parker S, Cartier N. Adeno-associated virus-based gene therapy for CNS diseases. Hum Gene Ther 2016; 27(7): 478-96. http://dx.doi.org/10.1089/hum.2016.087 PMID: 27267688
- [9] Wu Z, Asokan A, Samulski RJ. Adeno-associated virus serotypes: vector toolkit for human gene therapy. Mol Ther 2006; 14(3): 316-27.
- http://dx.doi.org/10.1016/j.ymthe.2006.05.009 PMID: 16824801
 [10] Sargeant TJ, Wang S, Bradley J, *et al.* Adeno-associated virus-mediated expression of β-hexosaminidase prevents neuronal loss in the Sandhoff mouse brain. Hum Mol Genet 2011; 20(22): 4371-80.
- http://dx.doi.org/10.1093/hmg/ddr364 PMID: 21852247

 [11] Cachón-González MB, Wang SZ, McNair R, *et al.* Gene transfer corrects acute GM2 gangliosidosis-potential therapeutic contribution of perivascular enzyme flow. Mol Ther 2012; 20(8):
 - http://dx.doi.org/10.1038/mt.2012.44 PMID: 22453766
- [12] Cachón-González MB, Wang SZ, Lynch A, Ziegler R, Cheng SH, Cox TM. Effective gene therapy in an authentic model of Tay-Sachs-related diseases. Proc Natl Acad Sci USA 2006; 103(27): 10373-8.
- http://dx.doi.org/10.1073/pnas.0603765103 PMID: 16801539
 [13] Bradbury AM, Cochran JN, McCurdy VJ, *et al.* Therapeutic response in feline sandhoff disease despite immunity to intracranial gene therapy. Mol Ther 2013; 21(7): 1306-15.

http://dx.doi.org/10.1038/mt.2013.86 PMID: 23689599

- [14] Cachón-González MB, Wang SZ, Ziegler R, Cheng SH, Cox TM. Reversibility of neuropathology in Tay-Sachs-related diseases. Hum Mol Genet 2014; 23(3): 730-48. http://dx.doi.org/10.1093/hmg/ddt459 PMID: 24057669
- [15] Bourgoin C, Emiliani C, Kremer EJ, et al. Widespread distribution of beta-hexosaminidase activity in the brain of a Sandhoff mouse model after coinjection of adenoviral vector and mannitol. Gene Ther 2003; 10(21): 1841-9. http://dx.doi.org/10.1038/sj.gt.3302081 PMID: 12960974

- [16] Mastakov MY, Baer K, Xu R, Fitzsimons H, During MJ. Combined injection of rAAV with mannitol enhances gene expression in the rat brain. Mol Ther 2001; 3(2): 225-32. http://dx.doi.org/10.1006/mthe.2001.0246 PMID: 11237679
- [17] Brown RC, Egleton RD, Davis TP. Mannitol opening of the blood-brain barrier: regional variation in the permeability of sucrose, but not 86Rb+ or albumin. Brain Res 2004; 1014(1-2): 221-7. http://dx.doi.org/10.1016/j.brainres.2004.04.034 PMID: 15213006
- [18] Carty N, Lee D, Dickey C, et al. Convection-enhanced delivery and systemic mannitol increase gene product distribution of AAV vectors 5, 8, and 9 and increase gene product in the adult mouse brain. J Neurosci Methods 2010; 194(1): 144-53. http://dx.doi.org/10.1016/j.jneumeth.2010.10.010 PMID: 20951738
- [19] Walia JS, Altaleb N, Bello A, et al. Long-term correction of Sand-hoff disease following intravenous delivery of rAAV9 to mouse neonates. Mol Ther 2015; 23(3): 414-22. http://dx.doi.org/10.1038/mt.2014.240 PMID: 25515709
- [20] Niemir N, Rouvière L, Besse A, et al. Intravenous administration of scAAV9-Hexb normalizes lifespan and prevents pathology in Sandhoff disease mice. Hum Mol Genet 2018; 27(6): 954-68. http://dx.doi.org/10.1093/hmg/ddy012 PMID: 29325092
- [21] Osmon KJ, Woodley E, Thompson P, et al. Systemic gene transfer of a hexosaminidase variant using an scAAV9.47 vector corrects GM2 gangliosidosis in sandhoff mice. Hum Gene Ther 2016; 27(7): 497-508. http://dx.doi.org/10.1089/hum.2016.015 PMID: 27199088
- [22] Tropak MB, Yonekawa S, Karumuthil-Melethil S, et al. Construction of a hybrid β-hexosaminidase subunit capable of forming stable homodimers that hydrolyze GM2 ganglioside in vivo. Mol Ther Methods Clin Dev 2016; 3: 15057. http://dx.doi.org/10.1038/mtm.2015.57 PMID: 26966698
- [23] Kyrkanides S, Miller JH, Brouxhon SM, Olschowka JA, Federoff HJ. beta-hexosaminidase lentiviral vectors: transfer into the CNS via systemic administration. Brain Res Mol Brain Res 2005; 133(2): 286-98. http://dx.doi.org/10.1016/j.molbrainres.2004.10.026 PMID: 15710246
- [24] Guidotti JE, Mignon A, Haase G, et al. Adenoviral gene therapy of the Tay-Sachs disease in hexosaminidase A-deficient knock-out mice. Hum Mol Genet 1999; 8(5): 831-8. http://dx.doi.org/10.1093/hmg/8.5.831 PMID: 10196372
- [25] Martino S, Marconi P, Tancini B, et al. A direct gene transfer strategy via brain internal capsule reverses the biochemical defect in Tay-Sachs disease. Hum Mol Genet 2005; 14(15): 2113-23. http://dx.doi.org/10.1093/hmg/ddi216 PMID: 15961412
- [26] Rockwell HE, McCurdy VJ, Eaton SC, et al. AAV-mediated gene delivery in a feline model of Sandhoff disease corrects lysosomal storage in the central nervous system. ASN Neuro 2015; 7(2): 1759091415569908. Available from: http://www.ncbi.nlm.nih.gov/pmc/articles/PMC4720176/http://dx.doi.org/10.1177/1759091415569908 PMID: 25873306
- [27] McCurdy VJ, Rockwell HE, Arthur JR, et al. Widespread correction of central nervous system disease after intracranial gene therapy in a feline model of Sandhoff disease. Gene Ther 2015; 22(2): 181-9.
- http://dx.doi.org/10.1038/gt.2014.108 PMID: 25474439

 [28] Gray-Edwards HL, Randle AN, Maitland SA, Benatti HR, Hubbard SM, Canning PF. Adeno-associated virus gene therapy in a sheep model of tay-sachs disease. Hum Gene Ther 2018; 29(3): 312-26.

 PMID: 28922945
- [29] Karumuthil-Melethil S, Nagabhushan Kalburgi S, Thompson P. Novel vector design and hexosaminidase variant enabling self-complementary adeno-associated virus for the treatment of Tay-Sachs disease. Hum Gene Ther 2016; 27(7): 509-21. http://dx.doi.org/10.1089/hum.2016.013 PMID: 27197548
- [30] Woodley E, Osmon KJL, Thompson P, et al. Efficacy of a bicistronic vector for correction of Sandhoff disease in a mouse model. Mol Ther Methods Clin Dev 2018; 12: 47-57. http://dx.doi.org/10.1016/j.omtm.2018.10.011 PMID: 30534578
- [31] Arfi A, Bourgoin C, Basso L, et al. Bicistronic lentiviral vector corrects beta-hexosaminidase deficiency in transduced and cross-

- corrected human Sandhoff fibroblasts. Neurobiol Dis 2005; 20(2): 583-93. http://dx.doi.org/10.1016/j.nbd.2005.04.017 PMID: 15953731
- [32] Igdoura SA, Mertineit C, Trasler JM, Gravel RA. Sialidase-mediated depletion of GM2 ganglioside in Tay-Sachs neuroglia cells. Hum Mol Genet 1999; 8(6): 1111-6. http://dx.doi.org/10.1093/hmg/8.6.1111 PMID: 10332044
- [33] Gray SJ, Matagne V, Bachaboina L, Yadav S, Ojeda SR, Samulski RJ. Preclinical differences of intravascular AAV9 delivery to neurons and glia: a comparative study of adult mice and nonhuman primates. Mol Ther 2011; 19(6): 1058-69. http://dx.doi.org/10.1038/mt.2011.72 PMID: 21487395
- [34] McCown TJ. Adeno-associated virus (AAV) vectors in the CNS. Curr Gene Ther 2005; 5(3): 333-8. http://dx.doi.org/10.2174/1566523054064995 PMID: 15975010
- [35] Thomas CE, Ehrhardt A, Kay MA. Progress and problems with the use of viral vectors for gene therapy. Nat Rev Genet 2003; 4(5): 346-58. http://dx.doi.org/10.1038/nrg1066 PMID: 12728277
- [36] Duque S, Joussemet B, Riviere C, et al. Intravenous administration of self-complementary AAV9 enables transgene delivery to adult motor neurons. Mol Ther 2009; 17(7): 1187-96. http://dx.doi.org/10.1038/mt.2009.71 PMID: 19367261
- [37] Foust KD, Nurre E, Montgomery CL, Hernandez A, Chan CM, Kaspar BK. Intravascular AAV9 preferentially targets neonatal neurons and adult astrocytes. Nat Biotechnol 2009; 27(1): 59-65. http://dx.doi.org/10.1038/nbt.1515 PMID: 19098898
- [38] Büning H, Perabo L, Coutelle O, Quadt-Humme S, Hallek M. Recent developments in adeno-associated virus vector technology. J Gene Med 2008; 10(7): 717-33. http://dx.doi.org/10.1002/jgm.1205 PMID: 18452237
- [39] Sango K, McDonald MP, Crawley JN, et al. Mice lacking both subunits of lysosomal β-hexosaminidase display gangliosidosis and mucopolysaccharidosis. Nat Genet 1996; 14(3): 348-52. http://dx.doi.org/10.1038/ng1196-348 PMID: 8896570
- [40] Sango K, Yamanaka S, Hoffmann A, et al. Mouse models of Tay-Sachs and Sandhoff diseases differ in neurologic phenotype and ganglioside metabolism. Nat Genet 1995; 11(2): 170-6. http://dx.doi.org/10.1038/ng1095-170 PMID: 7550345
- [41] Jackson laboratory B6;129S4-Hexb tm1Rlp/J. Availalble from: https://www.jax.org/strain/002914 [Cited 2019 Mar 6]
- [42] Gray SJ, Nagabhushan Kalburgi S, McCown TJ, Jude Samulski R. Global CNS gene delivery and evasion of anti-AAV-neutralizing antibodies by intrathecal AAV administration in non-human primates. Gene Ther 2013; 20(4): 450-9. http://dx.doi.org/10.1038/gt.2012.101 PMID: 23303281
- [43] Osmon KJL, Vyas M, Woodley E, Thompson P, Walia JS. Battery of behavioral tests assessing general locomotion, muscular strength, and coordination in mice. J Vis Exp 2018; (131): e55491-1.
- http://dx.doi.org/10.3791/55491 PMID: 29443024
 [44] Maegawa GHB, Tropak M, Buttner J, et al. Pyrimethamine as a potential pharmacological chaperone for late-onset forms of GM2 gangliosidosis. J Biol Chem 2007; 282(12): 9150-61. http://dx.doi.org/10.1074/jbc.M609304200 PMID: 17237499
- [45] Tropak MB, Reid SP, Guiral M, Withers SG, Mahuran D. Pharmacological enhancement of β-hexosaminidase activity in fibroblasts from adult Tay-Sachs and Sandhoff Patients. J Biol Chem 2004; 279(14): 13478-87. http://dx.doi.org/10.1074/jbc.M308523200 PMID: 14724290
- [46] Gray SJ, Blake BL, Criswell HE, et al. Directed evolution of a novel adeno-associated virus (AAV) vector that crosses the seizure-compromised blood-brain barrier (BBB). Mol Ther 2010; 18(3): 570-8.
- http://dx.doi.org/10.1038/mt.2009.292 PMID: 20040913

 [47] Folch J, Lees M, Sloane Stanley GH. A simple method for the isolation and purification of total lipides from animal tissues. J Biol Chem 1957; 226(1): 497-509.

 http://dx.doi.org/10.1016/S0021-9258(18)64849-5 PMID: 13428781
- [48] Folch J, Ascoli I, Lees M, Meath JA, LeBARON N. Preparation of lipide extracts from brain tissue. J Biol Chem 1951; 191(2): 833-41.

- http://dx.doi.org/10.1016/S0021-9258(18)55987-1 PMID: 14861228
- [49] Tropak MB, Bukovac SW, Rigat BA, Yonekawa S, Wakarchuk W, Mahuran DJ. A sensitive fluorescence-based assay for monitoring GM2 ganglioside hydrolysis in live patient cells and their lysates. Glycobiology 2010; 20(3): 356-65. http://dx.doi.org/10.1093/glycob/cwp183 PMID: 19917668
- [50] Wherrett JR, Cumings NJ. Detection and resolution of gangliosides in lipid extracts by thin-layer chromatography. Biochem J 1963; 86(2): 378-82. http://dx.doi.org/10.1042/bj0860378 PMID: 14000254
- [51] Yamada T, Bando H, Takeuchi S, et al. Genetically engineered humanized anti-ganglioside GM2 antibody against multiple organ metastasis produced by GM2-expressing small-cell lung cancer cells. Cancer Sci 2011; 102(12): 2157-63. http://dx.doi.org/10.1111/j.1349-7006.2011.02093.x PMID: 21895875
- [52] Suzuki K, Proia RL, Suzuki K. Mouse models of human lysoso-mal diseases. Brain Pathol 1998; 8(1): 195-215. http://dx.doi.org/10.1111/j.1750-3639.1998.tb00145.x PMID: 9458176
- [53] Phaneuf D, Wakamatsu N, Huang J-Q, et al. Dramatically different phenotypes in mouse models of human Tay-Sachs and Sandhoff diseases. Hum Mol Genet 1996; 5(1): 1-14. http://dx.doi.org/10.1093/hmg/5.1.1 PMID: 8789434
- [54] Pulicherla N, Shen S, Yadav S, et al. Engineering liver-detargeted AAV9 vectors for cardiac and musculoskeletal gene transfer. Mol Ther 2011; 19(6): 1070-8. http://dx.doi.org/10.1038/mt.2011.22 PMID: 21364538
- [55] Hinderer C, Katz N, Buza EL, et al. Severe toxicity in nonhuman primates and piglets following high-dose intravenous administration of an adeno-associated virus vector expressing human SMN. Hum Gene Ther 2018; 29(3): 285-98. http://dx.doi.org/10.1089/hum.2018.015 PMID: 29378426
- [56] Golebiowski D, van der Bom IMJ, Kwon C-S, et al. Direct intracranial injection of AAVrh8 encoding monkey β-N-acetylhex-osaminidase causes neurotoxicity in the primate brain. Hum Gene Ther 2017; 28(6): 510-22. http://dx.doi.org/10.1089/hum.2016.109 PMID: 28132521
- [57] Walkley SU, Vanier MT. Pathomechanisms in lysosomal storage disorders. Biochim Biophys Acta 2009; 1793(4): 726-36. http://dx.doi.org/10.1016/j.bbamcr.2008.11.014 PMID: 19111580
- [58] Fandino W. Understanding the physiological changes induced by mannitol: From the theory to the clinical practice in neuroanaesthesia. J Neuroanaesth Crit Care 2017; (4): 138-46. http://dx.doi.org/10.4103/jnacc.jnacc_31_17
- [59] Archer DP, Freymond D, Ravussin P. Utilisation du mannitol en neuroanesthésie et neuroréanimation. Ann Fr Anesth Reanim 1995; 14(1): 77-82. http://dx.doi.org/10.1016/S0750-7658(05)80154-6 PMID: 7677291
- [60] Winkler SR, Munoz-Ruiz L. Mechanism of action of mannitol. Surg Neurol 1995; 43(1): 59. http://dx.doi.org/10.1016/0090-3019(95)80039-J PMID: 7701425
- [61] McCarty DM, DiRosario J, Gulaid K, Muenzer J, Fu H. Mannitol-facilitated CNS entry of rAAV2 vector significantly delayed the neurological disease progression in MPS IIIB mice. Gene Ther 2009; 16(11): 1340-52. http://dx.doi.org/10.1038/gt.2009.85 PMID: 19587708
- [62] Foley CP, Rubin DG, Santillan A, et al. Intra-arterial delivery of AAV vectors to the mouse brain after mannitol mediated blood brain barrier disruption. J Control Release 2014; 196: 71-8. http://dx.doi.org/10.1016/j.jconrel.2014.09.018 PMID: 25270115
- [63] Donsante A, Vogler C, Muzyczka N, et al. Observed incidence of tumorigenesis in long-term rodent studies of rAAV vectors. Gene Ther 2001; 8(17): 1343-6. http://dx.doi.org/10.1038/sj.gt.3301541 PMID: 11571571
- [64] Russell DW. AAV vectors, insertional mutagenesis, and cancer. Mol Ther 2007; 15(10): 1740-3. http://dx.doi.org/10.1038/sj.mt.6300299 PMID: 17882145
- [65] Bell P, Moscioni AD, McCarter RJ, et al. Analysis of tumors arising in male B6C3F1 mice with and without AAV vector delivery to liver. Mol Ther 2006; 14(1): 34-44.

- http://dx.doi.org/10.1016/j.ymthe.2006.03.008 PMID: 16682254
 Chandler RJ, LaFave MC, Varshney GK, et al. Vector design influences hepatic genotoxicity after adeno-associated virus gene therapy. J Clin Invest 2015; 125(2): 870-80.
 http://dx.doi.org/10.1172/JCI79213 PMID: 25607839
- [67] Ruan C, Liu L, Wang Q, et al. Reactive oxygen species-biodegradable gene carrier for the targeting therapy of breast cancer. ACS Appl Mater Interfaces 2018; 10(12): 10398-408. http://dx.doi.org/10.1021/acsami.8b01712 PMID: 29498264

DISCLAIMER: The above article has been published, as is, ahead-of-print, to provide early visibility but is not the final version. Major publication processes like copyediting, proofing, typesetting and further review are still to be done and may lead to changes in the final published version, if it is eventually published. All legal disclaimers that apply to the final published article also apply to this ahead-of-print version.